arXiv:1510.07280v1 [q-fin.ST] 25 Oct 2015

Uncovering the evolution of non-stationary stochastic variables: the example of asset volume-price fluctuations

Paulo Rocha,[1,2] Frank Raischel,[3] João P. Boto,[1,2] and Pedro G. Lind[4,5]

[1]*Centro de Matemática e Aplicações Fundamentais Avenida Professor Gama Pinto 2, 1649-003 Lisboa, Portugal*
[2]*Departamento de Matemática, Faculdade de Ciências,*
University of Lisbon Campo Grande, Edifício C6, Piso 2, 1749-016 Lisboa, Portugal
[3]*Center for Geophysics, IDL, University of Lisbon 1749-016 Lisboa, Portugal*
[4]*ForWind - Center for Wind Energy Research, Institute of Physics,*
Carl-von-Ossietzky University of Oldenburg, DE-26111 Oldenburg, Germany
[5]*Institut für Physik, Universität Osnabrück, Barbarastrasse 7, 49076 Osnabrück, Germany*

(Dated: November 28, 2015)

We present a framework for describing the evolution of stochastic observables having a non-stationary distribution of values. The framework is applied to empirical volume-prices from assets traded at the New York stock exchange. Using Kullback-Leibler divergence we evaluate the best model out from four biparametric models standardly used in the context of financial data analysis. In our present data sets we conclude that the inverse Γ-distribution is a good model, particularly for the distribution tail of the largest volume-price fluctuations. Extracting the time-series of the corresponding parameter values we show that they evolve in time as stochastic variables themselves. For the particular case of the parameter controlling the volume-price distribution tail we are able to extract an Ornstein-Uhlenbeck equation which describes the fluctuations of the largest volume-prices observed in the data. Finally, we discuss how to bridge from the stochastic evolution of the distribution parameters to the stochastic evolution of the (non-stationary) observable and put our conclusions into perspective for other applications in geophysics and biology.

PACS numbers: 89.65.Gh, 02.50.Fz, 05.45.Tp, 05.10.Gg,
Keywords: Non-stationary systems, Langevin equation, Stochastic evolution, New York stock market

I. INTRODUCTION AND MOTIVATION

When assessing the behaviour of one complex system, such as the ones described by stochastic time series, one typically tries to uncover the non-linear interactions and the strength of fluctuating forces by means of extracting an evolution equation from the data[1]. When the underlying value-distributions of the observables are stationary, such approach is, in principle, possible[2]. However, in real systems the distributions are often either non-stationary or at least it is not possible to ascertain how reasonable the assumption of stationarity is.

In this paper we address the evolution of non-stationary value-distributions of stochastic observables and describe a framework that enables one to derive their evolution directly from measurements of empirical data recordings. We apply our framework to financial asset volume-prices, though the framework is general enough for many other systems as we also discuss in the end. In particular, we show that volume-price distributions evolve in a non-stationary way, but follow a typical functional shape, properly parametrized. By keeping track of the series of parameter values at each time-step, we show that they follow a well defined stochastic evolution equation, which helps to establish the evolution of the non-stationary distribution. It is known that even power-laws may be derived from stochastic equations driven by Gaussian noise[3].

The choice of considering volume-prices distributions as an example is not arbitrary. There is an old Wall Street adage which says that "*It takes volume to move price*"[4]. This adage holds still today. Indeed, if one considers volume or price separately from each other, one fails to grasp the behaviour of the capital exchanged which combines both variables. Therefore we consider here both variables combined, namely the volume-price, which measured the total capital exchanged, providing information about the entire capital traded in the market.

Several articles have been written about stochastic volatility models [5–7] in order to attempt to characterize the dynamics of the stock prices returns. Such models have emerged due to the well established non-Gaussian character of financial time-series[8]. For instance, asymptotic behaviour consistent with a power-law decay can not only be found in price fluctuations but also in trading volumes[4, 9]. Here, we find a strong competition or coexistence between a Gaussian model (log-normal) and heavy-tails (inverse-Γ). By focusing in large fluctuations, one can extract valuable information about the dynamics of a complex system, such the financial markets. We show that volume-price distribution have heavy-tails in the region of highest values. For this region of the distribution, we discuss how to use these findings for deriving possible risk metrics of non-stationary variables.

We start in Sec. II by introducing four different biparametric models that are typically used in finance to fit the empirical data. In Sec. III we investigate which models suit the best, for explaining the empirical distributions, introducing one variant of the Kullback-Leibler divergence. In Sec. IV we uncover the time evolution of the non-stationary distribution of the volume-price based in a framework that enables one to extract a stochastic motion equation for the distribution parameters. This approach was used in the financial context recently[10] when accessing clustering states of the stock

market[11]. In Sec. V we use our results to derive the evolution equations for the original non-stationary variable. Finally, in VI, we put our approach in perspective and discuss possible application in other situations, before summarizing the main conclusions of this paper.

II. NON-STATIONARY MODELS FOR STOCHASTIC VARIABLES

Some of the most typical statistical models for stochastic variables in different fields, ranging from physics[12, 13] and biology[14, 15] to finance[16] , medicine[17, 18] and even sociology among other fields[19], are biparametric. Moreover they account for a range where a polynomial Ansatz dominates and another which behaves exponentially. Four of the most used of such biparametric distributions are the $\Gamma-$distribution,

$$p_\Gamma(s) = \frac{s^{\phi_\Gamma - 1}}{\theta_\Gamma^{\phi_\Gamma}\Gamma[\phi_\Gamma]} exp\left[-\frac{s}{\theta_\Gamma}\right], \qquad (1)$$

the inverse Γ-distribution,

$$p_{1/\Gamma}(s) = \frac{\theta_{1/\Gamma}^{\phi_{1/\Gamma}}}{\Gamma[\phi_{1/\Gamma}]} s^{-\phi_{1/\Gamma}-1} exp\left[-\frac{\theta_{1/\Gamma}}{s}\right], \qquad (2)$$

the log-normal distribution,

$$p_{\ln}(s) = \frac{1}{\sqrt{2\pi}\theta_{\ln} s} exp\left[-\frac{(\log s - \phi_{\ln})^2}{2\theta_{\ln}^2}\right], \qquad (3)$$

and the Weibull distribution

$$p_W(s) = \frac{\phi_W}{\theta_W^{\phi_W}} s^{\phi_W - 1} exp\left[-\left(\frac{s}{\theta_W}\right)^{\phi_W}\right]. \qquad (4)$$

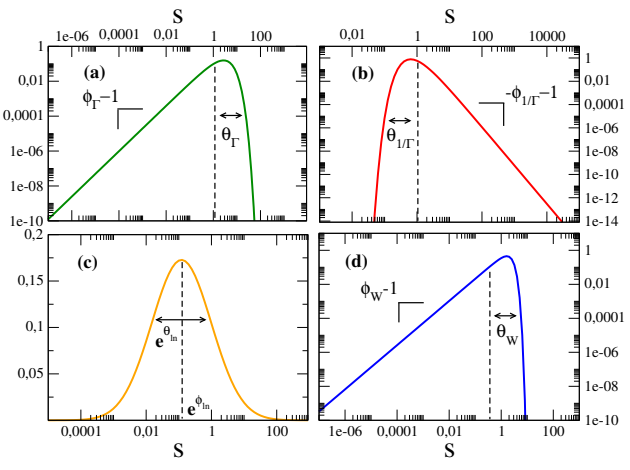

FIG. 1: (Color online) The four biparametric distributions in Eqs. (1)-(4): **(a)** the Γ-distribution, **(b)** the inverse Γ-distribution, **(c)** the log-normal distribution and **(d)** the Weibull distribution. For each model, a graphic illustration of its parameters is sketched.

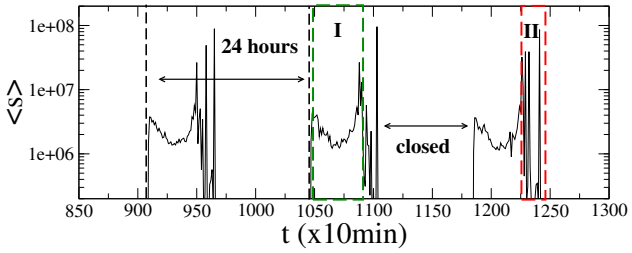

FIG. 2: (Color online) Illustration of the time-series of the average volume-price $\langle s \rangle$ of one company listed in the NYSE during a period of approximately three days. Here, (I) highlights the eight-hour period of normal trading and (II) the after-hours trading period (after closing), which is discarded from our analysis. During the night (non trading period) we set $s = 0$.

Next, we consider all these four distributions as candidate models for our data.

In each case one has two parameters, here represented by ϕ and θ, with a specific meaning. In the Γ-distribution ϕ_Γ characterize the left power-tail and θ_Γ accounts for the decaying time of the right-hand side as indicated in Fig. 1a. In the inverse Γ-distribution $\phi_{1/\Gamma}$ characterize the right power-tail and $\theta_{1/\Gamma}$ accounts for the decaying time of the left-hand side of the distribution as indicated in Fig. 1b. In the log-normal distribution ϕ_{ln} accounts for the mean and θ_{ln} for the standard deviation of the variables logarithm, as indicated in Fig. 1c. In the Weibull distribution ϕ_W characterizes the left power-tail, when the exponential term goes to one and θ_W accounts for the decaying of the right side of the distribution as indicated in Fig. 1d.

In the following we will analyze the volume-price (s) series of around 2000 companies having listed shares in the New York Stock Exchange (NYSE), with a sampling frequency of ten minutes, during a total of 976 days, which, after removing all the after-hours trading and discarding all the days with recording errors[20], contains around 1.8×10^4 data points. See illustration in Fig. 2. All the data were collected from the website `http://finance.yahoo.com/` and more details concerning its preprocessing may be found in Refs. [20, 21]. Also note that in Fig. 2 it is possible to observed a "U"-pattern, typically found in intraday volume time series[22].

In order to fit the empirical distribution of volume-price we use the least square scheme. We fit the empirical cumulative density function (CDF) of each one of the four models above. The cumulative distribution was used because of the smaller error associated when fitting the distributions tail. Figures 3a and 3b show respectively the probability and cumulative density function of each model (lines) that fit the empirical distribution (bullets) at one particular ten-minute snapshot.

In the case one considers the distributions in Eqs. (1) to (4) to be stationary, the parameters of each distribution are taken to be constants. In the following we introduce a different assumption: while we take a constant functional shape, i.e. one of the particular forms above, the corresponding parameters are allowed to vary in time, between two successive ten-minute snapshots. In other words, we assume that for the

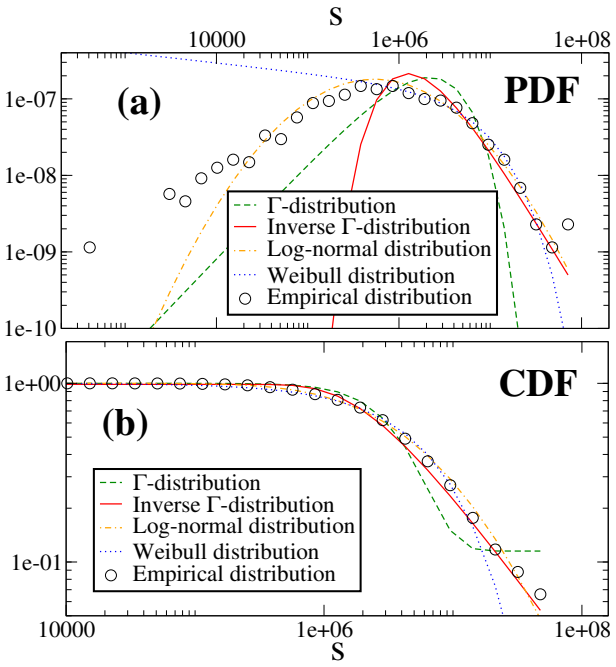

FIG. 3: (Color online) Illustration of the volume-price s distribution at one particular ten-minute snapshot: **(a)** Probability density function (PDF) and **(b)** cumulative density function (CDF). Different colors correspond to different models used to fit the empirical data (circles).

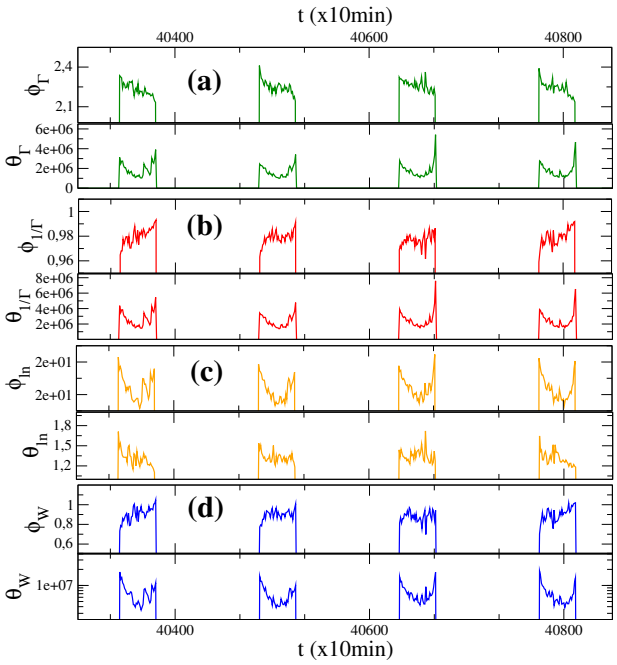

FIG. 4: (Color online) Time series of the two parameters characterizing the evolution of the cumulative density function (CDF) of the volume-price s: **(a)** Γ-distribution **(b)** inverse Γ-distribution, **(c)** log-normal distribution and **(d)** Weibull distribution. Each point in these time series correspond to ten-minute intervals. Periods with no activity correspond to the period where market is closed, and therefore will not be considered in our approach. In all plots, different colours correspond to different distributions.

general case of a non-stationary distribution or density function, the parameters ϕ and θ of the four models above are in fact variables of the distribution itself that include all the time dependency. In Fig. 4, we have a representation of the resulting time-series of each parameter, ϕ and θ, characterizing the four models (1-4).

III. SEARCHING FOR AN OPTIMAL MODEL OF VOLUME-PRICE DISTRIBUTIONS

In this section, we ascertain which model described previously is the best for the empirical set of volume-prices. To that end, we evaluate how accurate is the fit of each model using a "distance" between the empirical distribution and the modelled one, which we define as:

$$D^{(F)}(P||Q) = \sum_i \left| \ln\left(\frac{P(i)}{Q(i)}\right) \right| F(i)\Delta s_i \,, \qquad (5)$$

where $Q(i)$ is the empirical distribution, $P(i)$ is the modelled PDF and $F(i)$ is a weighting function. For $F(i) = P(i)$ one obtains the standard Kullback-Leibler divergence[23]. Figure 5a shows the rankings of all four models, evaluated according to the Kullback-Leibler divergence. As we can see, the best fit is the log-normal distribution, but not always. In a significant amount of 10-minute time-spans, the Weibull distribution retrieves the best fit.

Because of the choice for the weighting function $F(i) = P(i)$, the Kullback-Leibler divergence accounts for a good

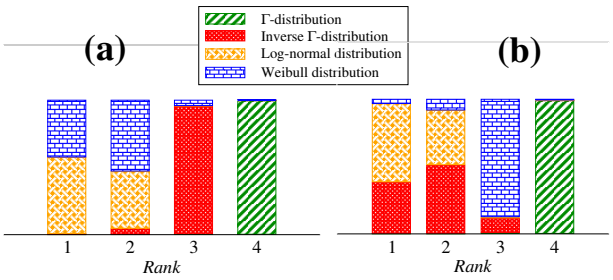

FIG. 5: (Color online) What is the best model? Ranking of the four distributions in Eqs. (1-4) used to fit the empirical data in two cases: **(a)** using the Kullback-Leibler divergence $D^{(p)}$, i.e. $F(i) = P(i)$ in Eq. (5) and **(b)** weighting the extreme events stronger, with a different distance $D^{(1/p)}$ with $F(i) = 1/P(i)$. In the first case, the full range of observed values was taken, in the second case only the volume-prices larger than the median were considered. Rank 1 indicates the best model.

fit in the central region, which is heavier weighted than the tails. In several situations however, the tails play a fundamental role. In the case of stock market volume-prices the tail in the range of large values is associated to the largest fluctuations, i.e. the largest gains and losses. Therefore, it can be the case that only this range of values is of importance. For accounting for the largest range of values one needs a proper weighting function that, in the following, we choose

	$D^{(P)}$		$D^{(1/P)}$	
	Average	Std Dev.	Average	Std Dev.
Γ-distribution	0.55	0.09	18	10
Inverse Γ-distribution	0.36	0.07	**0.9**	**0.6**
Log-normal	**0.2**	**0.4**	**1**	**1**
Weibull	**0.23**	**0.08**	3	3

TABLE I: Average and standard deviation for Kullback-Leibler divergence $D^{(p)}$ and for the tail distance $D^{(1/p)}$ (see text).

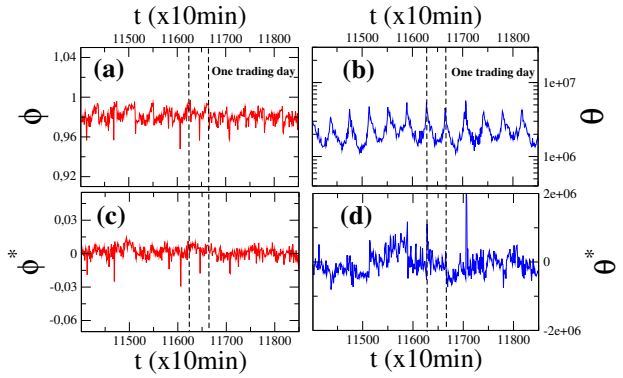

FIG. 6: (Color online) Illustration of the time-series of **(a)** ϕ (red) and **(b)** θ (blue), both parameters of the inverse Γ-distribution in Eq. (2). In **(c)** and **(d)** the corresponding detrended time-series, ϕ^* and θ^*, are plotted (see text). In this figure are roughly 13 trading days.

to be $F(i) = 1/P(i)$.

Figure 5b shows the ranking for this tail Kullback-Leibler divergence $D^{1/p}$. The results are now significantly different: the best models are the log-normal and the inverse Γ-distributions. When considering the tails, there is therefore a coexistence of log-normal and inverse-Γ.

Table I shows the mean value and standard deviation of the value distributions of the Kullback-Leibler divergence $D^{(p)}$ and of the tail distance $D^{(1/p)}$ for all 10-minute time-spans. For the tail, though the rank 1 is dominated by the log-normal distribution, the inverse Γ-distribution shows the smaller average distance $\langle D^{(1/p)} \rangle \sim 0.86$. Moreover, the inverse Γ-distribution is parametrized in a way that one single parameter, $\phi_{1/\Gamma}$, controls the tail of the largest values. Check Eq. (2) and Fig. 1b. For these reasons we choose henceforth the inverse Γ-distribution as our model for the evolution of the volume-price distribution tail.

IV. STOCHASTIC EVOLUTION OF THE DISTRIBUTION TAILS

In this section we extract the stochastic evolution of the distribution tail, choosing the inverse Γ-distribution as model. For simplicity we will only write ϕ and θ for the parameters $\phi_{1/\Gamma}$ and $\theta_{1/\Gamma}$.

For the analysis we will first study the average time-

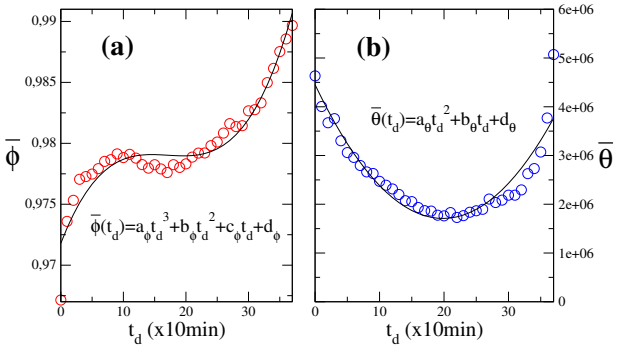

FIG. 7: (Color online) Average over all trading days of parameters ϕ and θ. Here we see that $\bar{\phi}$ seems to follow a cubic curve wile $\bar{\theta}$ seems to follow quadratic law. In the fitting function $\bar{\phi}(t_d)$ the coefficients have the value: $a_\phi = 1.55 \times 10^{-6}$, $b_\phi = -7.97 \times 10^{-5}$, $c_\phi = 1.33 \times 10^{-3}$ and $d_\phi = 9.72 \times 10^{-1}$. In the fitting function $\bar{\theta}(t_d)$ the coefficients have the value: $a_\theta = 6.97 \times 10^3$, $b_\theta = -2.77 \times 10^5$ and $c_\theta = 4.45 \times 10^6$ (see text).

evolution of each parameter during one single day. Indeed, as we can see from Fig. 6a and 6b, there is clearly a daily pattern $\bar{\phi}$ and $\bar{\theta}$, which after removed from the original series, yields the detrended data series of fluctuations, ϕ^* and θ^*, shown in Figs. 6c and 6d respectively. Our Ansatz is therefore defined by the decomposition of the original parameter series into their daily pattern and their fluctuations:

$$\phi(t) = \bar{\phi}(t) + \phi^*(t)\,, \tag{6a}$$
$$\theta(t) = \bar{\theta}(t) + \theta^*(t)\,. \tag{6b}$$

Since the series is non-stationary, we consider average daily patterns for a set of 20 days. The series of fluctuations were extracted by removing the 20-day moving average pattern from the original series. This was made by centring the windows in each point of the original series and subtracting the average of the points on ten days before and after that event.

Figure 7 shows the daily pattern of each parameter, where one sees the cubic dependence of ϕ on the time of the day, and the corresponding quadratic dependence of θ:

$$\bar{\phi}(t_d) = a_\phi t_d^3 + b_\phi t_d^2 + c_\phi t_d + d_\phi\,, \tag{7a}$$
$$\bar{\theta}(t_d) = a_\theta t_d^2 + b_\theta t_d + c_\theta\,, \tag{7b}$$

where $t_d = (t \pmod{1440}) - 540$ (in minutes). Note that the market is only open for normal trading during 6h30min (39×10min), this implies that outside of the normal trading period we define the $\bar{\phi}$ and $\bar{\theta}$ to be zero.

Next, we derive the evolution of parameter fluctuations, i.e. of the detrended variables ϕ^* and θ^*. The goal is to extract two stochastic differential equations that describe their evolution[2].

Figure 8a and 8b show the marginal probability density functions (PDF) of the variables ϕ and θ, which can be compared with the detrended variables separately (Figs. 8c and 8d). Clearly, the detrending does not have a significative effect on the shape of the PDF of these two parameters. Figure 8e shows the joint PDF of ϕ^* and θ^*. Here we see that

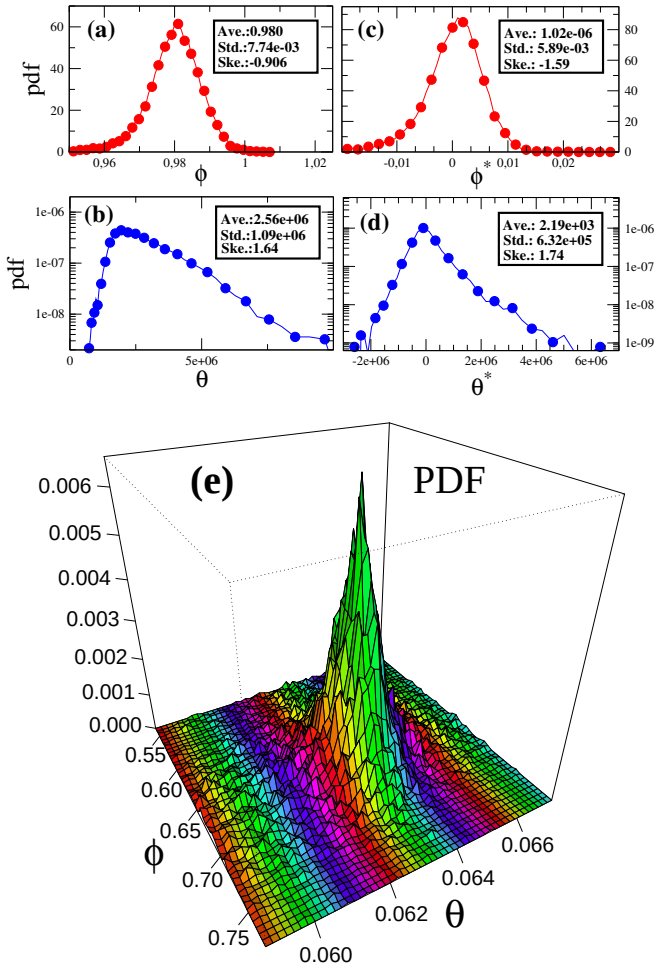

FIG. 8: (Color online) Probability density function (PDF) of the fitting parameters **(a)** ϕ and **(b)** θ, before the detrend, compared to the PDFs of their fluctuations **(c)** ϕ^* and **(d)** θ^*, after detrending (see text). In **(e)** one plots the joint PDF of both detrended variables ϕ^* and θ^*: both detrended variables can be taken as independent from one another (see text).

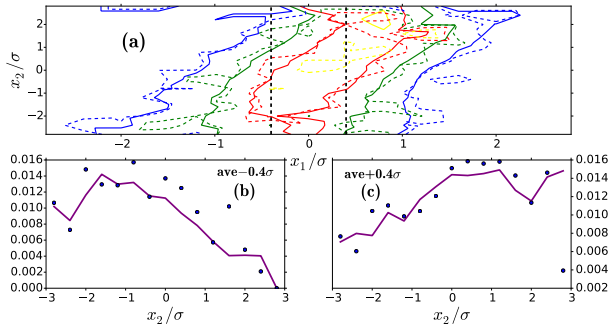

FIG. 9: (Color online) **(a)** Contour plots of the conditional PDF $p(x_1,\tau_1|x_2,\tau_2)$ (solid lines) and $p(x_1,\tau_1|x_2,\tau_2;x_3 = 0,\tau_3)$ (dashed lines) for $\tau_1 = \tau_{\min}$, $\tau_2 = 6\tau_{\min}$ and $\tau_3 = 12\tau_{\min}$, with $\tau_{\min} = 10$ min. The dashed vertical lines at $\langle x_1\rangle \mp 0.4\sigma$ indicates the cut shown in **(b)** and **(c)** respectively.

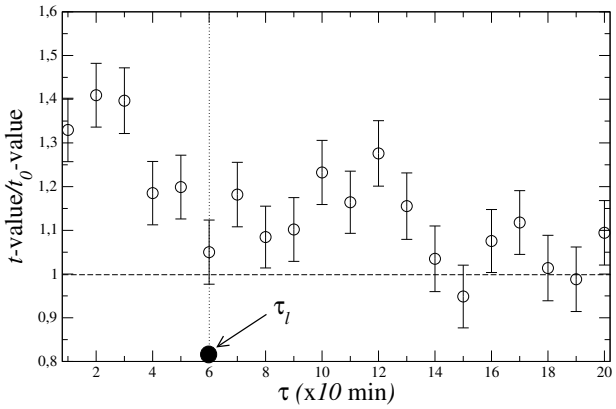

FIG. 10: Wilcoxon test to verify the Markovian property of ϕ^* time-series, showing the Markov length of $\tau_l = 60$ min.

these two parameters seem to be independent. Therefore we consider two uncoupled stochastic equation, one for each detrended variable. Moreover, since the observed fluctuations of θ do not play a significant role in the distribution tail, we approximate parameter θ by its daily pattern, $\theta(t) \sim \bar{\theta}(t_d)$.

Under these assumptions, to fully derive the evolution equations of both parameters (Eqs. (6)) one only needs to define additionally the fluctuations $\phi^*(t)$ which will be modelled according to the Langevin process

$$d\phi^* = D_1(\phi^*)dt + \sqrt{D_2(\phi^*)}dW_t\,. \qquad (8)$$

where $D_1(\phi^*)$ and $D_2(\phi^*)$ are the so called drift and diffusion coefficients respectively and dW_t is one Wiener process satisfying $\langle dW_t\rangle = 0$ and $\langle dW_t dW'_t\rangle = \delta(t-t')$.

A necessary ingredient of this approach is that ϕ^*-series must be Markovian. In order to test the Markov property we compute the transition probabilities $p(x_1,\tau_1|x_2,\tau_2)$ and $p(x_1,\tau_1|x_2,\tau_2;x_3 = 0,\tau_3)$. In Fig. 9a we show the contour plot of these two probabilities for $\tau_1 = \tau_{\min}$, $\tau_2 = 6\tau_{\min}$ and $\tau_3 = 12\tau_{\min}$, with $\tau_{\min} = 10$ min. The proximity of the contour lines suggest that the Markovian property holds. Moreover, in Fig. 9b and 9c, two cuts through the conditional probability densities are provided for fixed values of x_1, namely at $\langle x_1\rangle \pm 0.4\sigma$ which also seems to support this statement.

In order to create a quantitative understanding of whether or not the two conditional probabilities $p(x_1,\tau_1|x_2,\tau_2)$ and $p(x_1,\tau_1|x_2,\tau_2;x_3 = 0,\tau_3)$ are equal, the Wilcoxon rank-sum test[24] is employed. The value of t-value$/t_0$-value $= 1$ indicates that the process is Markovian. As we can see in Fig. 10, this test seems to further confirm that a proper Markov length is $\tau_l = 60$ min.

For a Markovian stochastic process, the evolution of the associated stochastic variable is defined by the two functions in Eq. (8), namely D_1 and D_2 given by:

$$D_k(\phi^*) = \lim_{\tau\to 0}\frac{M_k(\phi^*,\tau)}{k!\tau} \sim \frac{M_k(\phi^*,\tau_l)}{k!\tau_l}\,, \qquad (9)$$

for $k = 1, 2$ and where the conditional moments $M_k(x,\tau)$ are

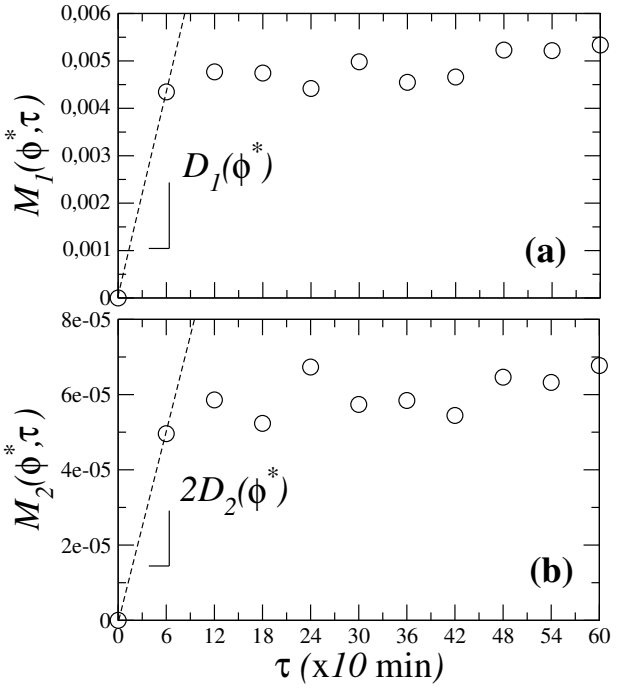

FIG. 11: Conditional moments extracted from the time-series of ϕ^*. **(a)** First conditional moment M_1 and **(b)** Second conditional moment M_2, both as functions of τ in units of 10 min.

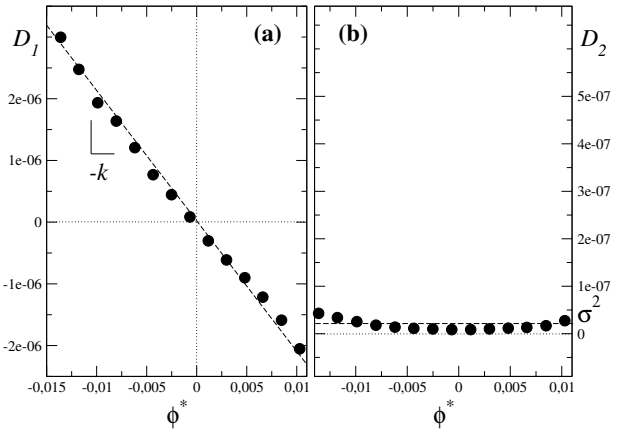

FIG. 12: Here we see that **(a)** the drift coefficient is linear in ϕ^* while **(b)** the diffusion coefficient can be consider constant. This two coefficients characterize the stochastic evolution of the parameter ϕ that describes the tail of the inverse Γ-distribution.

defined as:

$$M_k(\phi^*,\tau) = \left\langle \left(X_{t+\tau} - X_t\right)^k \right\rangle_{X_t=\phi^*} . \tag{10}$$

In Figs. 11a and 11b we represent the conditional moments M_1 and M_2 respectively, as a function of τ. By computing the slopes of M_1 and M_2 for each bin in variable ϕ yields a complete definition of both the drift D_1 and the diffusion D_2 coefficients for the full range of observed ϕ^* values.

Figures 12a and 12b show the drift and diffusion respectively. While the diffusion term has an almost constant amplitude, the drift is linear on ϕ^* with a negative sloped. Therefore the evolution of ϕ^* follows Eq. (8) with:

$$D_1(\phi^*) \;=\; -k\phi^* , \tag{11a}$$
$$D_2(\phi^*) \;=\; \sigma^2 , \tag{11b}$$

which defines an Ornstein-Uhlenbeck process for ϕ^*[1].

V. ACCESSING THE EVOLUTION OF THE NON-STATIONARY VOLUME-PRICE

Two important considerations follow from our findings, which we address in this section.

The first one deals with the evolution of the original (non-detrended) ϕ parameter, following the assumption that the distribution inverse-Γ is the best model for the tail at the largest volume-prices. Indeed, from the results shown in Fig. 12 and Eqs. (11) the evolution of the fluctuations ϕ^* is governed by:

$$d\phi^* = -k\phi^* dt + \sigma dW_t , \tag{12}$$

where $k = 2.02 \times 10^{-4}$ s^{-1} is the inverse response time from the market to perturbations in the largest range of fluctuations and $\sigma = 1.34 \times 10^{-4}$ s$^{-1/2}$ measures typical variations of these fluctuations themselves. Notice that k corresponds to a response time $1/k = 5.0 \times 10^3$ s, i.e. about one hour and twenty minutes, a value close to the Markov length calculated in the previous section. The market responds to perturbations at a time-scale close to the time-scale at which parameter ϕ experiences stochastic variations.

As Fig. 13 indicates, the autocorrelation of ϕ^* does not follow a simple exponential decay, but presents two distinct short-term and long-term regimes. We apply our Markov approach in the intermediate regime, avoiding the non-Markovian properties of the short-time scale, which has an autocorrelation time of $\approx 1/k$ compatible with the proposed Ornstein-Uhlenbeck process.

According to Eq. (6a) we can now write the evolution equation for the parameter ϕ, according to $d\phi = d\bar{\phi} + d\phi^*$, which, from Eq. (12) reads:

$$d\phi = -k(\phi - \phi_f)dt + \sigma dW_t , \tag{13}$$

where ϕ_f is a fixed point depending only on the average tail slope $\bar{\phi}$:

$$\phi_f = \bar{\phi} + \frac{1}{k}\frac{d\bar{\phi}}{dt} . \tag{14}$$

Equation (13) enable us to quantify the fluctuations in the region of largest volume-prices. By integrating Eq. (13), we conclude that the PDF tail has a slope $-\phi - 1$ which oscillates stochastically around $-\phi_f - 1$ with an oscillation amplitude of $\sigma^2/(2k) = 4.4 \times 10^{-5}$. See Appendix A for the full derivation. Physically, since ϕ_f changes along the day, this tail oscillation is analogous to a double pendulum, one purely deterministic given by Eq. (14) and another stochastic with amplitude $\sigma^2/(2k)$. Consequently, as sketched in Fig. 14, one

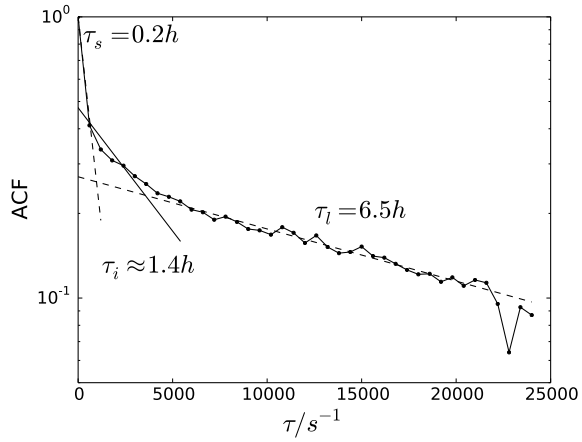

FIG. 13: Autocorrelation of ϕ^* as a function of delay τ. A short-term and a long-term regime exist, with autocorrelation times of $\tau_s \simeq 0.2$ hours and $\tau_l \simeq 6.5$ hours, respectively, with dashed lines indicating corresponding exponential fits. At the time scale of our Markov modelling, an intermediate scale $\tau_i = 1/k \simeq 1.4$ hours compatible with the time-scale of the Ornstein-Uhlenbeck process exists, with the continuous line representing its time scale.

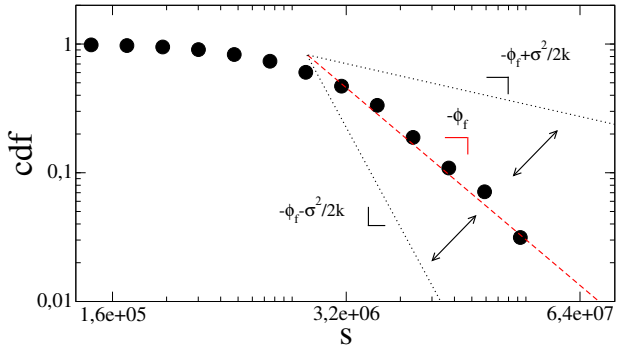

FIG. 14: (Color online) We have an harmonic restoring force mechanism due to the linear drift coefficient in the stochastic differential equation characterizing the evolution of the parameter ϕ.

can now establish an upper and lower bound for the tail of the empirical distribution, which may be helpful to derive risk measures for large fluctuations.

The second remarks deals with the description of the (non-stationary) evolution of the original stochastic variable, in this case the volume-price s. As we saw, while for the large-values tail the inverse-Γ model yields a good and simple description of its evolution, the log-normal distribution is found to be a good model for the tail as well for the central region of the volume-price distribution.

Also in this case the parameter ϕ and θ characterizing the log-normal distribution, Eq. (3), vary in time. Consequently, the well-defined distribution $P_{\phi,\theta}(s)$ parametrized by ϕ and θ which changes in time is now assumed to have all its time dependency incorporated in those two parameters. The log-normal model $P_{\phi,\theta}(s)$ could be taken as a model depending on the stochastic variable s and time t, $P(s, \phi(t), \theta(t))$.

If one is able to write all the moments of s as a function of the distribution parameters $\phi(t)$ and $\theta(t)$ one is able to fully characterize the non-stationary evolution of s. Indeed, the moments of s can be generally written as

$$\langle s^n \rangle = \int_0^{+\infty} s^n P(s, \phi(t), \theta(t)) ds \equiv F_n(\phi(t), \theta(t)) \,, \quad (15)$$

in case the integral exists. In the most general case, both parameters can be taken as stochastic variables coupled to each other, and therefore obeying the Langevin system of equations[2, 25]:

$$\begin{aligned} d\phi &= h_1(\phi,\theta)dt \\ &\quad + g_{11}(\phi,\theta)dW_1 + g_{12}(\phi,\theta)dW_2 \,, \end{aligned} \quad (16a)$$

$$\begin{aligned} d\theta &= h_2(\phi,\theta)dt \\ &\quad + g_{21}(\phi,\theta)dW_1 + g_{22}(\phi,\theta)dW_2 \,, \end{aligned} \quad (16b)$$

where $(h_1, h_2)^{(T)} = D_1$ and $gg^T = D_2$. Deriving function F in Eq. (15) one extracts the evolution equation of all statistical moments by differentiating Eq. (15) using Itô-Taylor expansion and incorporating the Eqs. (16), namely[25]

$$\begin{aligned} d\langle s^n \rangle &= A_n(\phi(t),\theta(t))dt + B_n(\phi(t),\theta(t))dW_1 \\ &\quad + C_n(\phi(t),\theta(t))dW_2 \end{aligned} \quad (17)$$

with

$$\begin{aligned} A_n(\phi(t),\theta(t)) &= \frac{\partial F_n}{\partial \phi} h_1 + \frac{\partial F_n}{\partial \theta} h_2 \\ &+ \frac{\partial^2 F_n}{\partial \phi \partial \theta}(g_{11}g_{21} + g_{12}g_{22}) \\ &+ \frac{1}{2}\frac{\partial^2 F_n}{\partial \phi^2}(g_{11}^2 + g_{12}^2) \\ &+ \frac{1}{2}\frac{\partial^2 F_n}{\partial \theta^2}(g_{21}^2 + g_{22}^2) \,, \end{aligned} \quad (18a)$$

$$B_n(\phi(t),\theta(t)) = \frac{\partial F_n}{\partial \phi} g_{11} + \frac{\partial F_n}{\partial \theta} g_{21} \,, \quad (18b)$$

$$C_n(\phi(t),\theta(t)) = \frac{\partial F_n}{\partial \phi} g_{12} + \frac{\partial F_n}{\partial \theta} g_{22} \,. \quad (18c)$$

Equation (17) is a stochastic differential equation with "drift" and "diffusion" functions which depend on time.

VI. DISCUSSION AND CONCLUSIONS

In this paper we study the stochastic evolution of the volume-price distributions of assets traded at the New York Stock Exchange as a prototypical example of non-stationary distributions of stochastic variables. We have shown that these distributions are non-stationary, in the sense that the parameters charactering the distribution are themselves stochastic variables. In order to find the best fit for the volume-price distribution we tested four bi-parametric models commonly

used in modelling the price of financial assets[16], namely: the Γ-distribution, inverse Γ-distribution, log-normal distribution and the Weibull distribution.

To weight each value in the volume-price spectrum according to some density function we introduced the tail Kullback-Leibler divergence, Eq. (5). Using this we showed that the inverse Γ-distribution seems a good model for accounting for region of the spectrum of highest values. Based on our findings, one can argue that the best model for the volume-price distributions may be a combination of a log-normal in the center of the distribution and a Pareto in the tails, known as a double Pareto log-normal distribution[26–29]. This aspect will be the subject of future investigation.

Moreover, attending to the fact that in the inverse Γ-distribution the two parameters decouple, we focus our study on the parameter ϕ, which characterizes the large fluctuations of volume-price distribution. By applying the framework in Ref. [2], we are able to extract a stochastic differential equation that describes the evolution of this parameter, Eq. (13), and permits the derivation of risk measures for the largest fluctuations.

We also provided a framework for deriving the stochastic evolution of a non-stationary variable, under the assumption that it follows a biparametric model whose parameters are themselves stochastic variables in time incorporating all the time dependency of the non-stationary process. By computing all the moments as a function of these distribution parameters, one is able to fully characterize the non-stationary evolution of the stochastic variable. In particular, this approach may be helpful in other situations and applications, such as in biology, when accessing the evolution of heart interbeat intervals or in energy sciences to address non-stationary measurement series in energy power production of wind turbines. These issues will also be considered in forthcoming studies.

Acknowledgments

The authors thank Philip Rinn and David Bastine for useful discussions and for providing the source code for the Wilcoxon test and the Langevin analysis. PR thanks *Fundação para a Ciência e a Tecnologia* and *Centro de Matemática e Aplicações Fundamentais* for financial support during the time of development of this project and *Deutscher Akademischer Austauschdienst* for the intership fellowship through IPID4all from University of Oldenburg. PR and JPB thanks *Faculdade de Ciências da Universidade de Lisboa* for providing working accommodation. FR thanks *Fundação para a Ciência e a Tecnologia* (FCT) for the fellowship SFRH/BPD/65427/2009. PGL thanks German Environment Ministry for financial support. PGL and FR thank *Deutscher Akademischer Austauschdienst* (DAAD) and FCT for support from bilateral collaboration DRI/DAAD/1208/2013.

Appendix A: The stochastic evolution of distribution tails

By extracting the coefficients D_1 and D_2 from the empirical data, one can write down a stochastic differential equation that characterizes the evolution of ϕ as in Eq. (13) , where ϕ_f is a fixed point, and k and σ are constants. This is also known as a Ornstein-Uhlenbeck process[30].

Integration of Eq. (13) follows as:

$$\begin{aligned}\phi &= \phi_0 e^{-k(t-t_0)} + \int_{t_0}^{t} e^{-k(t-s)} \left(k\phi_f ds + \sigma dW_s\right) \\ &= \phi_0 e^{-k(t-t_0)} + \phi_f \left(1 - e^{-k(t-t_0)}\right) \\ &\quad + \sigma \int_{t_0}^{t} e^{-k(t-s)} dW_s \,. \end{aligned} \tag{A1}$$

From Eq. (A1), the expected value of ϕ follows as

$$\mathbf{E}(\phi) = \mathbf{E}(\phi_0) e^{-k(t-t_0)} + \phi_f \left(1 - e^{-k(t-t_0)}\right) , \tag{A2}$$

and the corresponding variance is given by

$$\mathrm{Var}(\phi) = \mathbf{E}(\phi^2) - \mathbf{E}(\phi)^2 \tag{A3}$$

and substituting ϕ and $\mathbf{E}(\phi)$ by the right-hand side of Eqs. (A1) and (A2).

$$\begin{aligned}\mathrm{Var}(\phi) &= \mathbf{E}\Bigg(\left(\phi_0 e^{-k(t-t_0)} + \phi_f \left(1 - e^{-k(t-t_0)}\right)\right)^2 + 2\left(\phi_0 e^{-k(t-t_0)} + \phi_f \left(1 - e^{-k(t-t_0)}\right)\right)\left(\sigma \int_{t_0}^{t} e^{-k(t-s)} dW_s\right) \\ &\quad + \left(\sigma \int_{t_0}^{t} e^{-k(t-s)} dW_s\right)^2 \Bigg) - \mathbf{E}(\phi)^2 \\ &= \mathbf{E}\left(\left(\phi_0 e^{-k(t-t_0)} + \phi_f \left(1 - e^{-k(t-t_0)}\right)\right)^2 \right) + \mathbf{E}\left(\left(\sigma \int_{t_0}^{t} e^{-k(t-s)} dW_s\right)^2 \right) \\ &\quad - \left(\mathbf{E}(\phi_0) e^{-k(t-t_0)} + \phi_f \left(1 - e^{-k(t-t_0)}\right) \right)^2 \\ &= \mathbf{E}\left(\left(\sigma \int_{t_0}^{t} e^{-k(t-s)} dW_s\right)^2 \right) = \mathbf{E}\left(\sigma^2 \int_{t_0}^{t} \int_{t_0}^{t} e^{-k(t-s)} e^{-k(t-s')} \delta(s-s') ds ds' \right)\end{aligned}$$

$$= \mathbf{E}\left(\sigma^2 e^{-2kt}\int_{t_0}^{t}\int_{t_0}^{t} e^{ks}e^{ks'}\delta(s-s')dsds'\right) = \mathbf{E}\left(\sigma^2 e^{-2kt}\int_{t_0}^{t} e^{2ks}ds\right)$$
$$= \frac{\sigma^2}{2k}\left(1-e^{-2k(t-t_0)}\right). \tag{A4}$$

For long times, $t \to +\infty$, one arrives to

$$\mathbf{E}(\phi) \to \phi_f \tag{A5}$$

and

$$\mathrm{Var}(\phi) \to \frac{\sigma^2}{2k}. \tag{A6}$$

[1] H. Risken, *Fokker-Planck Equation* (Springer, Berlin, 1984).
[2] R. Friedrich, J. Peinke, M. Sahimi, and M. Tabar, Phys. Rep. **506**, 87 (2011).
[3] J. Ruseckas and B. Kaulakys, Phys. Rev. E **81**, 031105 (2010).
[4] P. Gopikrishnan, V. Plerou, X. Gabaix, and H. E. Stanley, Phys. Rev. E **62** (2000).
[5] D. Delpini and G. Bormetti, Phys. Rev. E **83**, 041111 (2011).
[6] J. F. Muzy, R. Baïle, and E. Bacry, Phys. Rev. E **87**, 042813 (2013).
[7] M. Zamparo, F. Baldovin, M. Caraglio, and A. L. Stella, Phys. Rev. E **88**, 062808 (2013).
[8] A. Gerig, J. Vicente, and M. A. Fuentes, Phys. Rev. E **80**, 065102(R) (2009).
[9] X. Gabaix, P. Gopikrishnan, V. Plerou, and H. Stanley, Nature **423**, 267270 (2003).
[10] P. Rinn, Y. Stepanov, J. Peinke, T. Guhr, and R. Schäfer, Europhysics Letters **110**, 68003 (2015).
[11] M. Münnix, T. Shimada, R. Schäfer, F. Leyvraz, T. Seligman, T. Guhr, and H. Stanley, Scientific Reports **2**, 644 (2012).
[12] J. H. Lienhard and P. L. Meyer, An. Math. Stat. **25** (1967).
[13] I. Eliazar, Phys. Rev. E **86**, 031103 (2012).
[14] P. Comtois, Aerobiologia **16**, 171 (2000).
[15] X. Xia, *Data Analysis in Molecular Biology and Evolution*, Vol. 1 (Kluwer Academic Publishers, North Carolina, 2002) p. 254.
[16] S. Camargo, S. M. D. Queirós, and C. Anteneodo, Eur. Phys. J. B **86**, 159 (2013).
[17] H. P. Zhu, X. Xia, C. H. Yu, A. Adnan, S. F. Liu, and Y. K. Du, BMC Gastroenterology **11** (2011).
[18] H. Shen, L. Brown, and H. Zhi, Statist. Med. **25**, 3023 (2006).
[19] E. Limpert, W. A. Stahel, and M. Abbt, BioScience **51**, 341 (2001).
[20] P. Rocha, F. Raischel, J. Cruz, and P. G. Lind, in *3rd SMTDA Conference Proceedings* (2015) pp. 619–627.
[21] P. Rocha, F. Raischel, J. Boto, and P. G. Lind, J. Phys.: Conf. Ser. **574**, 012148 (2014).
[22] A. R. Admati and P. Pleiderer, Review of Financial Studies **1**, 3 (1988).
[23] S. Kullback and R. Leibler, An. Math. Stat. **22**, 7986 (1951).
[24] F. Wilcoxon, Biometrics Bulletin **1**, 80 (1945).
[25] V. V. Vasconcelos, F. Raischel, M. Haase, J. Peinke, M. Wächter, P. G. Lind, and D. Kleinhans, Phys. Rev. E **84**, 031103 (2011).
[26] Z. Fang, J. Wang, B. Liu, and W. Gong, in *Handbook of Optimization in Complex Networks*, Springer Optimization and Its Applications, Vol. 57, edited by M. T. Thai and P. M. Pardalos (Springer US, 2012) pp. 55–80.
[27] K. Giesen, A. Zimmermann, and J. Suedekum, Journal of Urban Economics **68**, 129 (2010).
[28] M. Bee, *Statistical analysis of the Lognormal-Pareto distribution using Probability Weighted Moments and Maximum Likelihood*, Tech. Rep. 1208 (Department of Economics, University of Trento, Italia, 2012).
[29] W. J. Reed and M. Jorgensen, Communications in Statistics - Theory and Methods **33**, 1733 (2004).
[30] G. E. Uhlenbeck and L. S. Ornstein, Phys. Rev. **36**, 823 (1930).